$2.37\Gamma(k + 3/2)/k^{1/2}\Gamma(k + 1)$.

Modification of the theory of Yamakawa and Yoshizaki[10] for the intrinsic viscosity $[\eta]_R$ of a completely rigid rod macromolecule for a Schulz–Flory distribution of molecular weights provides an equation of the form[18]

$$[\eta]_R = [(k + 2)(k + 1)/k^2](\pi N_A \bar{L}_n^3/24M_n)g(k,d,\bar{L}_n)$$

where g is a very complicated relation which is cited elsewhere.[18] The ratio $[\eta]/[\eta]_R$, where $[\eta]$ is the intrinsic viscosity of semiflexible rods with the same contour length, can be expressed by an equation related to that given by those authors[10] which is a function of $\bar{L}_n/q$ and k.

It is possible also to modify the theory of Hagerman and Zimm[11] for the effect of partial flexibility on the rotational relaxation time τ_0 to take into account molecular weight distribution as described elsewhere.[18]

Registry No. Schizophyllan, 9050-67-3.

References and Notes

(1) Kikumoto, S.; Miyajima, T.; Yoshizumi, S.; Fujimoto, S.; Kimura, K. *J. Agric. Chem. Soc. Jpn.* **1970**, *44*, 337.
(2) Kikumoto, S.; Miyajima, T.; Kimura, K.; Okubo, S.; Komatsu, N. *J. Agric. Chem. Soc. Jpn.* **1971**, *45*, 162.
(3) Norisuye, T.; Yanaki, T.; Fujita, H. *J. Polym. Sci., Polym. Phys. Ed.* **1980**, *18*, 547.
(4) Kashiwagi, Y.; Norisuye, T.; Fujita, H. *Macromolecules* **1981**, *14*, 1220.
(5) Sato, T.; Norisuye, T.; Fujita, H. *Macromolecules* **1983**, *16*, 185.
(6) Warren, T. C.; Schrag, J. L.; Ferry, J. D. *Biopolymers* **1973**, *12*, 1905.
(7) Hvidt, S.; Ferry, J. D.; Roelke, D. L.; Greaser, M. L. *Macromolecules* **1983**, *16*, 740.
(8) Nestler, F. H. M.; Hvidt, S.; Ferry, J. D.; Veis, A. *Biopolymers* **1983**, *22*, 1747.
(9) Amis, E. J.; Carriere, C. J.; Ferry, J. D.; Veis, A. *Int. J. Biol. Macromol.* **1985**, *7*, 130.
(10) Yamakawa, H.; Yoshizaki, T. *Macromolecules* **1980**, *13*, 633.
(11) Hagerman, P. J.; Zimm, B. H. *Biopolymers* **1981**, *20*, 1481.
(12) Elias, H.-G. "Macromolecules"; Plenum Press: New York, 1977; Vol. 1, p 288.
(13) Schrag, J. L.; Johnson, R. M. *Rev. Sci. Instrum.* **1971**, *42*, 224.
(14) Nestler, F. H. M. Ph.D. Thesis, University of Wisconsin, 1981.
(15) Amis, E. J.; Carriere, C. J.; Nestler, F. H. M. Report No. 98, Rheology Research Center, University of Wisconsin, 1984.
(16) Zimm, B. H. *J. Chem. Phys.* **1956**, *24*, 269.
(17) Ookubo, N.; Komatsubara, M.; Nakajima, H.; Wada, Y. *Biopolymers* **1976**, *15*, 929.
(18) Carriere, C. J.; Amis, E. J.; Ferry, J. D. Report No. 100, Rheology Research Center, University of Wisconsin, 1985. Carriere, C. J. Ph.D. Thesis, University of Wisconsin, 1985.
(19) Broersma, S. *J. Chem. Phys.* **1960**, *32*, 1626.

Dynamic Rheology and Molecular Weight Distribution of Insoluble Polymers: Tetrafluoroethylene–Hexafluoropropylene Copolymers

Souheng Wu

Central Research and Development Department, E. I. du Pont de Nemours and Company, Experimental Station, Wilmington, Delaware 19898.

Received June 19, 1984

ABSTRACT: Dynamic melt viscoelasticity for four insoluble copolymers of tetrafluoroethylene and hexafluoropropylene of the same comonomer content but different molecular weights is measured and analyzed to obtain their molecular weight distribution curves by deconvolution of the dynamic modulus spectrum in the terminal and plateau zones. The results are also used to study the polymerization kinetics, polydispersity effects on steady-state compliance, and the relationship between zero-shear viscosity and molecular weight. It is found that the free radical dispersion polymerization proceeds essentially by binary coupling of growing chains. The steady-state compliance J_e° is related to the polydispersity ratio by $J_e^\circ = \{6/(5G_N^\circ)\}(M_z/M_w)^{3.7}$ for $M > M_c'$, where M_c' is the critical entanglement molecular weight for steady-state compliance, G_N° is the plateau modulus, and M_z and M_w are z-average and weight-average molecular weights. The zero-shear viscosity η_0 for $M > M_c$ is found to be given by $\eta_0 = \eta_0(M_c)(M/M_c)^3 \exp\{2.26(1 - (M_c/M)^{0.5}\}$, where $\eta_0(M_c)$ is the zero-shear viscosity at the critical entanglement molecular weight M_c for zero-shear viscosity. This relation is obtained by a modification of Doi–Edwards reptation theory for tube length fluctuation and indicates that the n in the power law $\eta_0 = \eta_0(M_c)(M/M_c)^n$ is not a constant but rather varies from 4.1 at $M = M_c$ and asymptotically decreases to 3 at $M \to \infty$. In the range $1 < M/M_c < 100$ typical for conventional polymers, the relation predicts $n = 3.5$ as the best least-squares fit, in agreement with the well-known empirical results.

Introduction

Recently, we developed a method for obtaining the molecular weight distribution of polymers by deconvolution of linear melt viscoelasticity in the terminal and plateau zones.[1,2] The method is applicable to insoluble as well as soluble polymers and was verified with a series of narrow- and broad-distribution polystyrenes.[1,2]

In this work, we apply the method to a series of tetrafluoroethylene–hexafluoropropylene copolymers (FEP), which are insoluble in any suitable solvents and whose molecular weight distributions cannot be determined by traditional methods such as light scattering, osmometry, and gel permeation chromatography. The results obtained are also used to analyze polymerization kinetics, the effect of polydispersity on steady-state compliance, and the relation between zero-shear viscosity and molecular weight.

Dynamic Theory and Methodology

The dynamic modulus spectrum of a polymer melt in the terminal and plateau zones contains a complete spectrum of molecular relaxation times, which can be deconvoluted to obtain the molecular weight distribution curve. The linear viscoelastic storage modulus for a polydisperse polymer is given by[1]

$$G'(\tau) = \int_{-\infty}^{\infty} D(\tau)\frac{8}{\pi^2}G_N^\circ \sum_{\text{odd } p}\frac{(1/p^2)(\omega\tau/p^2)^2}{1 + (\omega\tau/p^2)^2}\, d\log\tau \quad (1)$$

where $G'(\omega)$ is the dynamic storage modulus at angular

0024-9297/85/2218-2023$01.50/0

Table I
Composition and End Groups of FEP Fluoro Polymers

polymer	wt % HFP by FTIR[a]	T_g(DSC), °C	end groups by FTIR no. of equiv per 10^6 C atoms: COF	COOH	$CF{=}CF_2$	CF_2H	total	M_n from end groups
FEP 4	10.38	96	~0	2.3	27.8	137.2	167.3	6.29×10^5
FEP 3	9.87		0.7	6.3	30.2	209.8	247.0	4.26×10^5
FEP 2	10.41	96	4.0	4.9	40.5	316.7	366.1	2.87×10^5
FEP 1	10.77		1.1	4.0	22.9	396.1	424.1	2.48×10^5

[a] The average HFP content is 10.38 ± 0.32% by weight, or 7.2 ± 0.2% by mole.

Table II
Melting and Crystallization Behavior of FEP Fluoro Polymers by DSC[a]

polymer	T_m,[b] °C: peak	end	ΔH_f,[c] cal/g	% crystallinity from ΔH_f	T_c,[d] °C: peak	end	ΔH_c,[e] cal/g
FEP 4	264	274	3.85	17	246	241	2.92
FEP 3	268	278	4.49	20	249	245	5.00
FEP 2	267	276	4.76	21	251	244	3.04
FEP 1	262	275	4.56	21	253	242	5.33

[a] Heating and cooling rates are both 10 °C/min. [b] T_m = melting point [c] ΔH_f = heat of fusion. [d] T_c = crystallization point. [e] ΔH_c = heat of crystallization.

frequency ω, τ the tube disengagement time for a monodisperse species of molecular weight M in the polydisperse blend, G_N° the plateau modulus, $D(\tau)$ the weight-fraction differential molecular weight distribution function in τ scale, and p the odd integers. The kernel of eq 1 is the G' for monodisperse species given by the Doi–Edwards reptation theory.[3] Since each mode has an amplitude of $1/p^2$, the series converges rapidly, and only one to three terms are needed to represent the G' of monodisperse species adequately.[1] The tube disengagement time in a polydisperse blend τ is related to that in a monodisperse whole polymer τ_m by

$$\tau = \mu\tau_m \tag{2}$$

where μ accounts for the shift in the relaxation time of a monodisperse species in the polydisperse blend and may be expressed in terms of the friction coefficients.[1] μ is less than unity for species with $M > M_w$ and is greater than unity for species with $M < M_w$. This shift tends to narrow the relaxation time spectrum.

$D(\tau)$ can be transformed to the molecular weight scale by using the relation

$$\tau = \lambda M^\beta \tag{3}$$

where λ and β are numerical constants.[1] If there is no shift in relaxation times on blending (i.e., $\mu = 1$), we have $\beta = 2$ for $M/M_c < 1$ according to the Rouse theory,[4] $\beta = 3$ for $M/M_c > 50$ according to the Doi–Edwards theory,[3] and $\beta = 3.5$ for $1 < M/M_c < 50$ empirically and as shown later by considering tube leakage in the reptation theory. Generally, however, $\mu \neq 1$, and β tends to be smaller, reflecting the narrowing of the relaxation time spectrum due to the shift of the relaxation time in the polydisperse blend. In this work, we determine λ and β experimentally, discussed later.

The weight-fraction differential molecular weight distribution function is defined by

$$D(M) = \mathrm{d}W(M)/\mathrm{d}\log M \tag{4}$$

where $W(M)$ is the cumulative mass molecular weight distribution function, given by

$$W(M) = \int_{-\infty}^{\log M} D(M)\ \mathrm{d}\log M \tag{5}$$

To obtain $D(M)$, the experimental G' spectrum in the terminal and plateau zones is deconvoluted by eq 1 and then converted to the weight-fraction differential molecular weight distribution function by eq 3, as illustrated with polystyrenes before.[1] Good agreement of the present method with light scattering, osmometry, and gel permeation chromatography was demonstrated.

Materials

Four tetrafluoroethylene–hexafluoropropylene copolymers (FEP) of the same comonomer content (10.4 ± 0.3% by weight or 7.2 ± 0.2% by mole of HFP) but varying molecular weights, prepared by free radical dispersion polymerization, are used (Table I). The HFP content was determined by FTIR, and the T_g was found to be 96 °C by DSC, which agrees with the literature value determined by DMA at 1 Hz.[5]

End groups were determined by FTIR. Although there are some variations among the four FEPs, the various end groups are in the molar ratio COF:COOH:$CF{=}CF_2$:CF_2H = 0.4:1.6:11:87. The number-average molecular weights were calculated from the total number of end groups by

$$M_n = 105.2 \times 10^6/Q \tag{6}$$

where Q is the number of equivalents of end groups in 10^6 carbon atoms (Table I).

DSC shows that the crystalline melting point is about 265 °C and the crystallization temperature on cooling from the melt is about 245 °C (Table II).

Dynamic Modulus Spectra

The dynamic moduli G' and G'' were determined with the Rheometrics System 4 mechanical spectrometer at temperatures of 285, 300, 340, and 370 °C, using the cone and plate of 25-mm diameter with 0.1-rad cone angle. To ensure linear viscoelastic behavior, measurements were made at several different shear strains (usually 0.5–2% strain above 0.1 rad/s, 1–25% strain between 0.1 and 0.01 rad/s). The torque trace during the sinusoidal oscillation was also examined for conformance to the sine wave. The lowest temperature used was 285 °C to avoid residual crystallinity, and the highest temperature used was 370 °C to avoid thermal decomposition. Shear creep measurements were made to examine the thermal stability. It was found that sufficient thermal decomposition will occur to change the zero-shear viscosity, if the sample is aged at 370 °C for longer than 3 h. All rheological measurements were made well within this limit.

The G' and G'' were superimposed to obtain the master curves at the reference temperature of 340 °C (Figures 1–4). The shift factor is given by $a_T = (\eta_0/\eta_{00})(T_0\rho_0/T\rho)$,

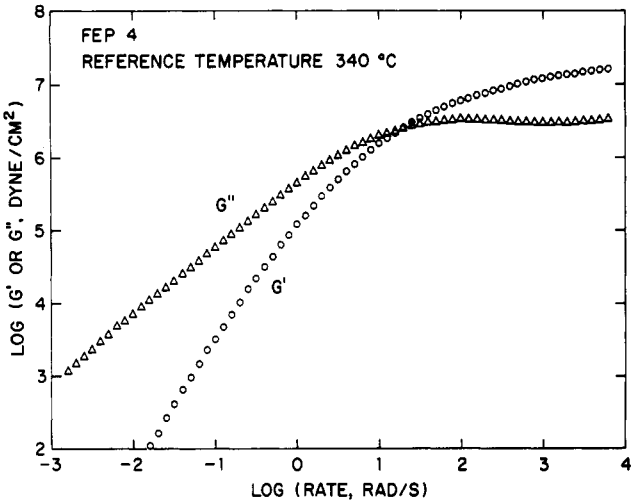

Figure 1. Dynamic modulus master curves at 340 °C for FEP 4.

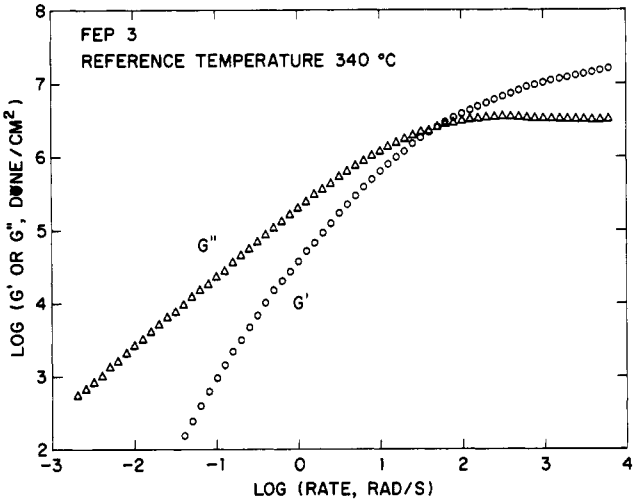

Figure 2. Dynamic modulus master curves at 340 °C for FEP 3.

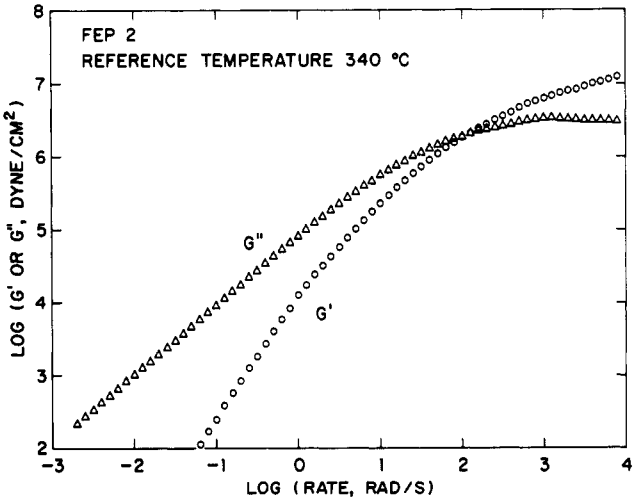

Figure 3. Dynamic modulus master curves at 340 °C for FEP 2.

where η_0 is the zero-shear viscosity at T, η_{00} is the zero-shear viscosity at the reference temperature T_0, and the density ρ is given by

$$1/\rho = 0.406 + 7.3 \times 10^{-4}t \quad (7)$$

where ρ is in g/mL and t is the temperature in °C.

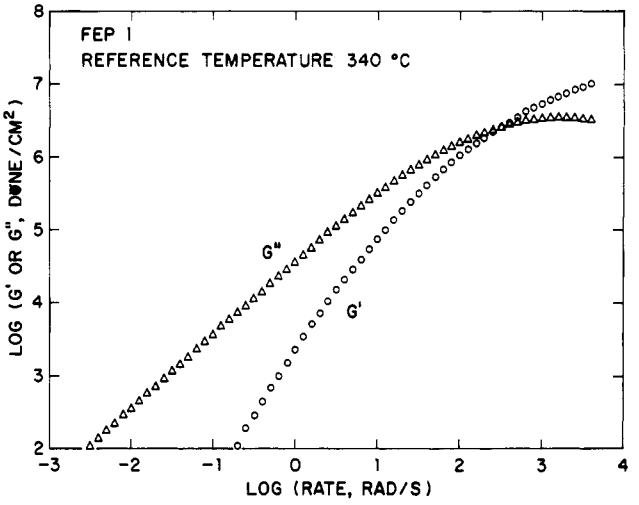

Figure 4. Dynamic modulus master curves at 340 °C for FEP 1.

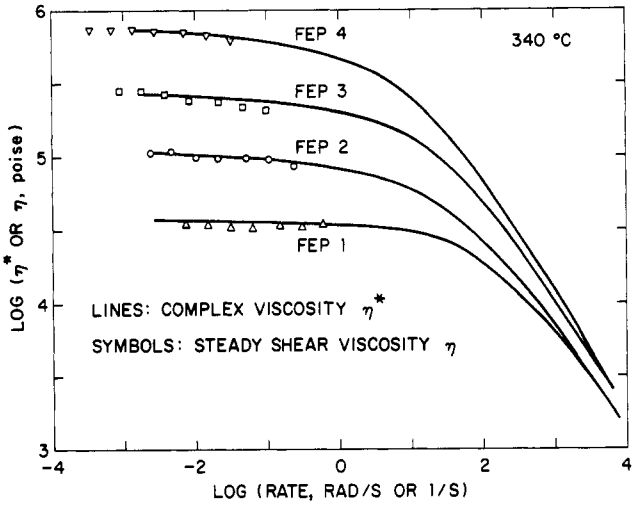

Figure 5. Viscosity vs. rate at 340 °C.

Table III
Zero-Shear Viscosity and Shift Factor for FEP Fluoro Polymers

polymer	temp,[a] °C	η_0, P	$a_T = \eta_0/\eta_{00}$
FEP 4	370	3.82×10^5	0.515
	340	7.41×10^5	1.000
	300	2.19×10^6	2.95
	285	4.18×10^6	5.64
FEP 3	370	1.38×10^5	0.487
	340	2.83×10^5	1.000
	300	8.91×10^5	3.15
	285	1.62×10^6	5.74
FEP 2	370	5.54×10^4	0.523
	340	1.06×10^5	1.000
	300	3.31×10^5	3.12
	285	5.70×10^5	5.38
FEP 1	370	1.46×10^4	0.432
	340	3.45×10^4	1.000
	300	1.18×10^5	3.41
	285	1.77×10^5	5.13

[a] Reference temperature T_0 = 340 °C.

The zero-shear viscosity was measured by creep under constant shear stress, using the cone and plate of 25-mm diameter and 0.1-rad cone angle with the Rheometrics stress rheometer. The results are plotted in Figure 5, together with the complex viscosity obtained from dynamic oscillation. As can be seen, the two methods agree quite well. The zero-shear viscosities and the shift factors are listed in Table III.

Table IV
Molecular Weights and Polydispersity Ratios for FEP Fluoro Polymers Determined by Dynamic Rheometry[a]

polymer	M_n by FTIR	M_n	M_w	M_z	M_{z+1}	M_{z+2}	M_{z+3}	M_{z+4}	M_w/M_n	M_z/M_w
FEP 4	6.29×10^5	6.074×10^5	9.565×10^5	1.534×10^6	2.396×10^6	3.326×10^6	4.052×10^6	4.336×10^6	1.575	1.604
FEP 3	4.26×10^5	4.525×10^5	6.605×10^5	9.734×10^5	1.413×10^6	1.895×10^6	2.295×10^6	2.490×10^6	1.460	1.474
FEP 2	2.87×10^5	2.677×10^5	4.348×10^5	7.155×10^5	1.144×10^6	1.608×10^6	1.965×10^6	2.053×10^6	1.624	1.646
FEP 1	2.48×10^5	2.620×10^5	3.565×10^5	4.888×10^5	6.780×10^5	9.042×10^5	1.112×10^6	1.267×10^6	1.360	1.371

[a] $M_e = 6.24 \times 10^3$; $M_c = 1.25 \times 10^4$; $M_c' = 4.37 \times 10^4$.

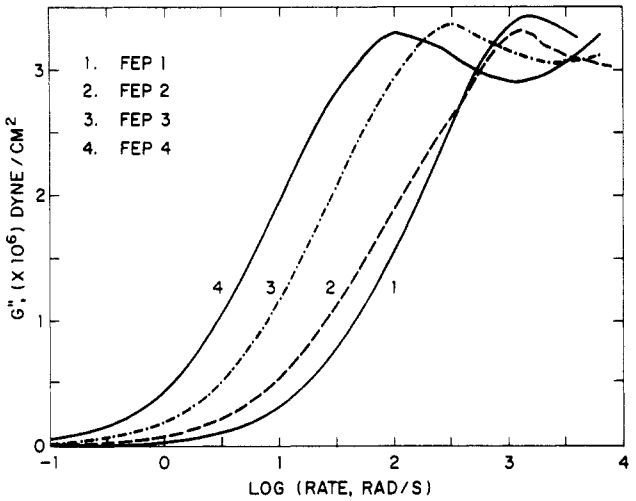

Figure 6. G'' vs. log ω at 340 °C for FEP fluoro polymers.

The shift factor is fitted to the WLF equation for a reference temperature of 340 °C (or 613 K) by Marquardt–Levenberg nonlinear least-squares iteration,[1] giving

$$\log a_T = 12.5379 - \frac{16.0(T - 369)}{67.9 + (T - 369)} \tag{8}$$

The numerical constants give $f_g = 0.027$ and $\alpha_f = 3.99 \times 10^{-4}$ K^{-1}, in good agreement with the "universal" values of $f_g = 0.025$ and $\alpha_f = 4.84 \times 10^{-4}$ K^{-1}, where f_g is the free-volume fraction at T_g and α_f the thermal expansion coefficient of the free volume. Alternatively, the shift factor is plotted in terms of the Arrhenius equation, giving an apparent activation energy for flow of $E_a = 20.5$ kcal/mol, which compares reasonably with the value of 18–36 kcal/mol for poly(tetrafluoroethylene)[6-9] and those for other polymers.[10,11]

The plateau modulus $G_N°$ was determined by[12-16]

$$G_N° = (4/\pi)\int_{-\infty}^{\omega_{max}} G'' \, d \ln \omega \tag{9}$$

where ω_{max} is the frequency at G''_{max}. Figure 6 shows the G'' vs. log ω plots for the four FEPs. Equation 9 gives an average value for the four FEPs as

$$G_N° = (1.25 \pm 0.03) \times 10^7 \text{ dyn/cm}^2 \tag{10}$$

It is interesting to note that the equation of Raju and co-workers,[16] $G_N° = 3.56G''_{max}$, gives $G_N° = (1.22 \pm 0.04) \times 10^7$ dyn/cm^2 for the present FEPs, in good agreement with the value obtained by eq 9.

The entanglement molecular weight M_e is calculated to be

$$M_e = \rho RT/G_N° = 6.24 \times 10^3 \tag{11}$$

indicating that the number of main-chain carbon atoms between entanglement points is 119, which is reasonable for flexible-chain polymers.[12,13]

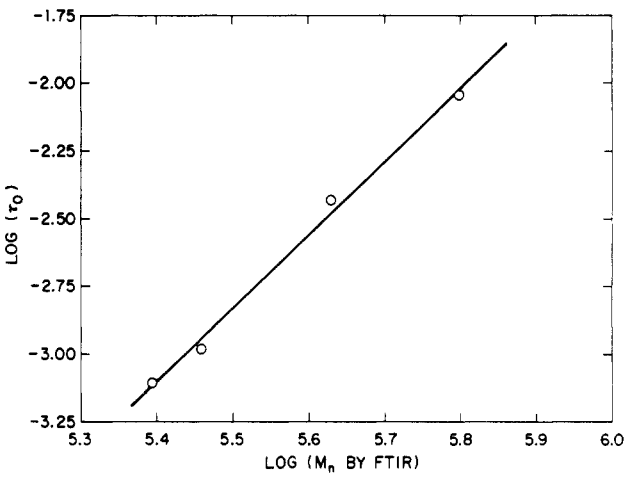

Figure 7. log τ_0 vs. log M_n for FEP fluoro polymers, where the M_n is determined by FTIR end-group analysis.

Molecular Weights and Distributions

The G' master curve in the terminal zone is fitted to the empirical relation[1]

$$G'(\omega)/G_N° = \frac{(\tau_0\omega)^c}{1 + (\tau_0\omega)^c} \tag{12}$$

where τ_0 is the characteristic relaxation time and c is a parameter characterizing the breadth of the relaxation time spectrum. The parameters τ_0 and c are determined by Marquardt–Levenberg nonlinear least-squares iteration. In the numerical calculation, $G'/G_N°$ is fitted as a function of log ω, as discussed before.[1] The weight-fraction differential molecular weight distribution function in the τ scale is obtained as[1]

$$D(\tau) = \left.\frac{(2/\pi)(1/\tau_0)(10)^{cx} \sin(\pi c/2)}{(1/\tau_0)^2(10)^{2cx} + (2/\tau_0)(10)^{cx}\cos(\pi c/2) + 1}\right|_{\tau=1/\omega} \tag{13}$$

where $x = \log \omega$. Equation 13 is obtained by inversion of eq 1.

To convert $D(\tau)$ from the τ scale to the M scale, we plot log τ_0 vs. log M_n, where M_n was determined from end groups, as shown in Figure 7, obtaining

$$\tau \propto M_n^{2.70} \tag{14}$$

This relationship is used to calculate $D(M)$ on a relative M scale. The relative number-average molecular weight $(M_n)_r$ thus obtained is next scaled to the absolute value by plotting $(M_n)_r$ vs. M_n, where the M_n was determined from the FTIR end groups (Table I). Least-squares regression gives

$$\log \tau = -17.926 + 2.70 \log M \tag{15}$$

which is used to obtain $D(M)$ on the absolute M scale. The differential weight-fraction molecular weight distribution curves are normalized to the total mass of 100 and are

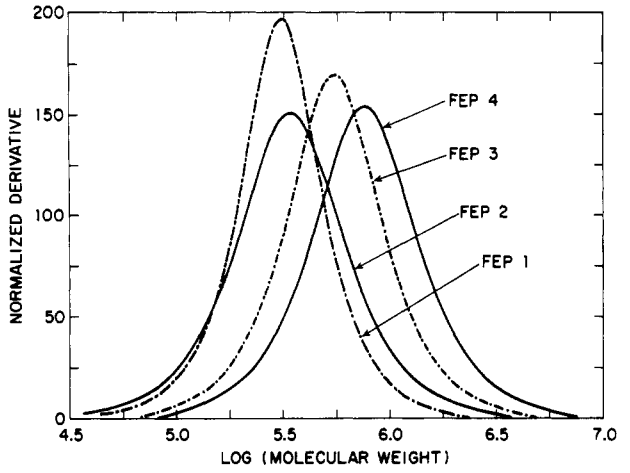

Figure 8. Weight-fraction differential molecular weight distribution curves for fluoro polymers by dynamic rheology.

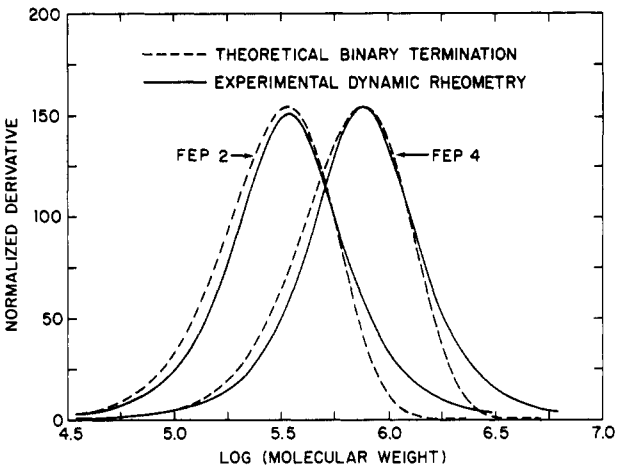

Figure 9. Comparison of experimental and theoretical binary coupling distribution curves for FEP 2 and FEP 4.

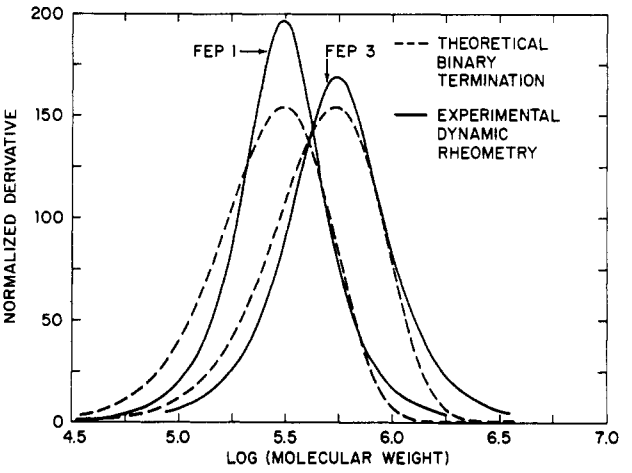

Figure 10. Comparison of experimental and theoretical binary coupling distributions for FEP 1 and FEP 3.

plotted in Figure 8. The various average molecular weights are listed in Table IV. The M_n determined by FTIR and the M_n determined by the present rheological method agree well.

Polymerization Kinetics

The present FEPs were prepared by free radical dispersion polymerization, as already mentioned. Comparison of the experimental molecular weight distribution curves with the theoretical Schulz–Flory distribution shows that the FEP polymerization proceeds essentially by binary coupling of growing chains, discussed below.

The Schulz–Flory distribution[17] assumes a steady-state condition that the number of growing chains is constant, and monomers are added randomly until the growth center of the chain is inactivated by termination. The individual chain growth centers need not all begin at the same time and need not remain active throughout the polymerization process. Free radical polymerization fits this type of process. The Schulz–Flory distribution is given by

$$dW/d\ln M = m^{k+1}M^{k+1}\{1/\Gamma(k+1)\}\exp(-mM) \qquad (16)$$

where W is the cumulative mass, $\Gamma(k+1)$ is the gamma function, k is the coupling constant, and $m = k/M_n$. For the "most probable" distribution, $k = 1$. For the binary coupling termination, $k = 2$. The various average molecular weights are related to one another by

$$M_n/k = M_w/(k+1) = M_z/(k+2) \qquad (17)$$

The M_w/M_n values for the present FEPs are all about 1.5, indicating that the polymerization kinetics is essentially by binary coupling termination ($k = 2$). This is further supported by comparing the molecular weight distribution curves with the Schulz–Flory distribution for binary coupling ($k = 2$), shown in Figures 9 and 10 for all four FEPs. The agreement between the experimental and the theoretical curves is quite reasonable. The actual distribution curves are however skewed somewhat toward the high molecular weight range with lesser amounts of low molecular weight fractions. This is probably because of the depletion of active growth centers and the decreased probability of chain coupling toward the end of polymerization process. This is consistent with the expectation that fluoro polymer radicals should be quite stable against abstraction and disproportionation. Therefore, the polymerization should proceed mainly by binary coupling termination, until the concentration of active centers is sufficiently depleted near the end of the process, when it gradually shifts toward the most probable distribution.

Polydispersity and Steady-State Compliance

The steady-state compliance J_e° is determined from the relaxation time spectrum $H(\tau)$ in the terminal zone by[13]

$$J_e^\circ = \frac{\int_{-\infty}^{\infty}\tau^2 H(\tau)\,d\ln\tau}{\left[\int_{-\infty}^{\infty}\tau H(\tau)\,d\ln\tau\right]^2} \qquad (18)$$

The results are listed in Table V.

For monodisperse polymers with $M < M_c'$, the J_e° is directly proportional to molecular weight, given by Rouse theory[4] as

$$J_e^\circ = (2/5)M/(\rho RT) \qquad \text{for } M < M_c' \qquad (19)$$

where M_c' is the critical molecular weight for entanglement coupling in J_e°, given by

$$M_c' \simeq 7M_e = 4.37 \times 10^4 \qquad (20)$$

for FEPs. On the other hand, for monodisperse polymers with $M > M_c'$, the J_e° is independent of molecular weight, given by Doi–Edwards theory[3,18] as

$$J_e^\circ G_N^\circ = 6/5 \qquad \text{for } M > M_c' \qquad (21)$$

However, experimental data on narrow-distribution polymers suggest an empirical relation[12,13]

$$J_e^\circ G_N^\circ = 3.6 \pm 0.8 \qquad \text{for } M > M_c' \qquad (22)$$

We show below that eq 21 appears to be indeed correct, while the higher value of eq 22 appears to arise from the

Table V
Steady-State Compliance and Polydispersity of FEP Fluoro Polymers[a]

polymer	exptl $J_e°$, cm²/dyn	calcd by Doi–Edwards theory, eq 23, using $J^* = 6/(5G_N°)$	calcd by Doi–Edwards theory, eq 23, using $J^* = 3.6/G_N°$	calcd by the Mills equation, eq 24, using $J^* = 6/(5G_N°)$	calcd by the Mills equation, eq 24, using $J^* = 3.6/G_N°$	calcd by the Zosel equation, eq 25, using $J^* = 6/(5G_N°)$	calcd by the Zosel equation, eq 25, using $J^* = 3.6/G_N°$
FEP 4	8.30×10^{-7}	15.9×10^{-7}	47.8×10^{-7}	7.82×10^{-7}	23.5×10^{-7}	4.18×10^{-7}	12.5×10^{-7}
FEP 3	7.31×10^{-7}	11.4×10^{-7}	34.3×10^{-7}	6.60×10^{-7}	19.9×10^{-7}	3.71×10^{-7}	11.1×10^{-7}
FEP 2	8.62×10^{-7}	17.5×10^{-7}	52.5×10^{-7}	8.27×10^{-7}	24.8×10^{-7}	4.34×10^{-7}	13.0×10^{-7}
FEP 1	5.10×10^{-7}	10.4×10^{-7}	31.1×10^{-7}	5.77×10^{-7}	17.3×10^{-7}	3.37×10^{-7}	10.1×10^{-7}

[a] $M_c' = 4.37 \times 10^4$.

presence of high molecular weight fractions in the samples used.

The polydispersity has a profound effect on $J_e°$. The Doi–Edwards theory predicts

$$J_e° = J^* \frac{M_{z+4}M_{z+3}M_{z+2}}{M_{z+1}M_zM_w} \quad \text{for } M > M_c' \qquad (23)$$

where $J^* = J_e°(M_c')$. On the other hand, a number of empirical equations have been proposed. Mills[19] proposed

$$J_e° = J^*(M_z/M_w)^{3.7} \quad \text{for } M > M_c' \qquad (24)$$

Zosel[20] proposed

$$J_e° = J^*(M_z/M_w)^{2.5} \quad \text{for } M > M_c' \qquad (25)$$

Several other relations have also been reviewed.[13] All indicate that $J_e°$ is quite sensitive to the high-moment molecular weights.

We test these relations as follows. All the present FEPs have $M_w > M_c'$. Combining eq 21 with eq 24 gives

$$J_e° = \{(6/5)/G_N°\}(M_z/M_w)^{3.7} \quad \text{for } M > M_c' \qquad (26)$$

that is using the Doi–Edwards theory for J^* and the Mills relation for polydispersity. Equation 26 is shown to predict the $J_e°$ correctly, whereas other combinations give poor results, as can be seen in Table V. Thus, the Doi–Edwards theory is correct for J^* but overestimates the polydispersity effect. The empirical equation 22 overestimates the J^* by a factor of about 3. The Mills equation is correct for the polydispersity effect, while the Zosel equation underestimates it.

Zero-Shear Viscosity and Molecular Weight Relationship

The zero-shear viscosity and molecular weight relationship can be written as

$$\eta_0 = \eta_0(M_c)(M/M_c)^n \qquad (27)$$

where $\eta_0(M_c)$ is the zero-shear viscosity of a Rouse chain at $M = M_c$ and n is a numerical constant. The M_c is the critical molecular weight for entanglement coupling in η_0 and is given by

$$M_c \simeq 2M_e = 1.25 \times 10^4 \qquad (28)$$

for FEPs. For $M < M_c$, Rouse theory[4] predicts $n = 1$, which has been confirmed experimentally at constant friction coefficients.[12,13,21] On the other hand, for $M > M_c$, empirically $n = 3.4$.[12,13,21] However, no existing theories predict such a relationship.

Recently, Graessley[18] and Doi[22] noted that the reptation theory can be written as

$$\eta_0 = 9.6\eta_0(M_c)(M/M_c)^3 \quad \text{for } M > M_c \qquad (29)$$

which predicts $n = 3$. Equation 29 is the Doi–Edwards equation, which overestimates the zero-shear viscosity at M_c by a factor of 9.6. However, at high molecular weights ($M/M_c > 50$), eq 29 and the empirical equation $\eta_0 = \eta_0(M_c)(M/M_c)^{3.4}$ merge together, as seen later. Graessley[18] thus suggested that $n = 3.4$ is only an approximation, valid in the conventional molecular weight range $1 < M/M_c < 50$, and the Doi–Edwards theory should be indeed correct for very high molecular weights, i.e., $M/M_c \gtrsim 50$.

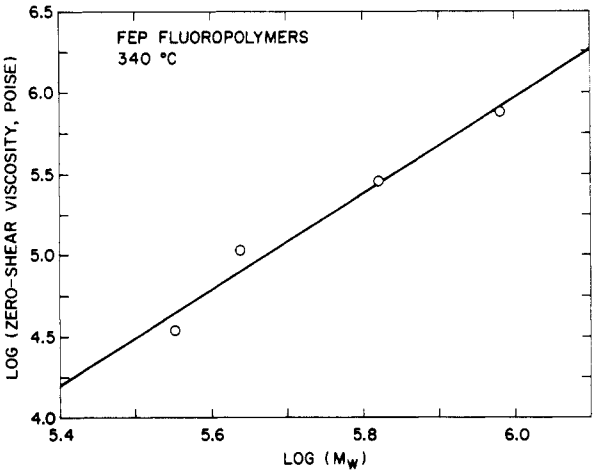

Figure 11. log η_0 vs. log M_w for FEPs at 340 °C. $M_w/M_c = 29$–77, and the slope by least squares is 2.94.

The present FEPs have very high molecular weights, having $M_w/M_c = 29$–77. Therefore, they provide an opportunity for testing Graessley's suggestion. Figure 11 plots log η_0 vs. log M_w at 340 °C for the four FEPs. Least-squares regression gives

$$\eta_0 = 2.04 \times 10^{-12}M_w^{2.94} \qquad (30)$$

The use of M_w for correlation with η_0 has been well established.[23-26] The n value of 2.94 is quite close to the theoretical value of 3, thus confirming the prediction of Doi–Edwards theory at very high molecular weights.

Thus, though applicable to very high molecular weights, the Doi–Edwards theory overestimates the η_0 in the conventional molecular weight ranges. This appears to be due to neglect of the tube length fluctuation.[22,27,28] We include this effect in the reptation model as below, obtaining an equation that correctly predicts $n = 3.5$ in the conventional molecular weight ranges, which gradually decreases to the asymptotic value of $n = 3$ at very high molecular weights.

Tube Length Fluctuation

The Doi–Edwards theory[3] considered the reptation of a Rouse chain but neglected its wriggling motion, which will cause the chain to leak out of the tube ends.[22] This provides a relaxation mechanism in addition to the reptation. This tube leakage effect can be assumed to be negligible for very long chains ($M/M_c > 50$) but is quite significant for shorter chains, typical for conventional polymers ($M/M_c = 1$–50). The tube contour length fluctuation due to the leakage is given by

$$\delta L = \{(L(t) - \bar{L})^2\}^{1/2} \simeq (M/M_e)^{0.5}\bar{L} \qquad (31)$$

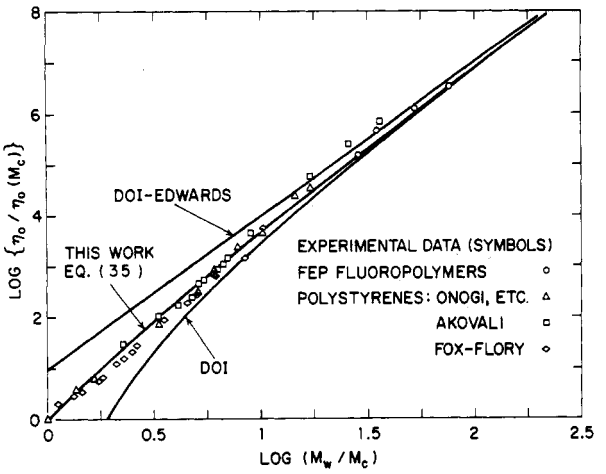

Figure 12. $\eta_0/\eta_0(M_c)$ vs. M_w/M_c master curve for $M/M_c > 1$, showing good agreement of eq 35 with experiment. Equation 35 is from this work. The Doi–Edwards equation is eq 29. The Doi equation is eq 32.

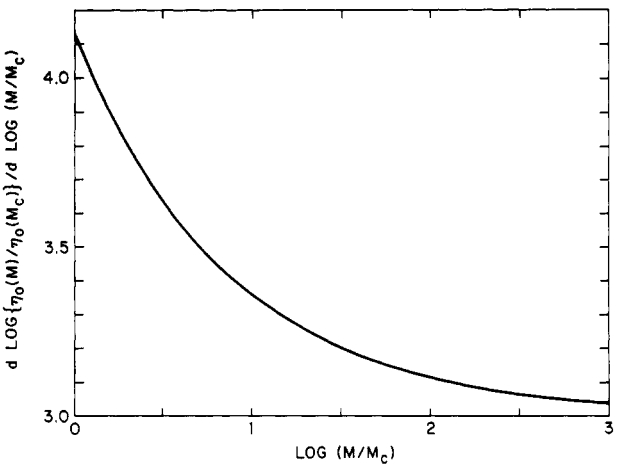

Figure 13. d log $\{\eta_0/\eta_0(M_c)\}$/d log (M/M_c) vs. M/M_c plot. Note that n = d log $\{\eta_0/\eta_0(M_c)\}$/d log (M/M_c) in the relation $\eta_0 = \eta_0(M_c)(M/M_c)^n$.

where $L(t)$ is the instantaneous tube contour length at time t, $\bar{L}$ the average tube contour length, and M/M_e the number of steps per chain. The time-average tube contour length is $\{L(t)\} \equiv \bar{L} = (M/M_e)a$, where a is the entanglement mesh size. Equation 31 indicates that if $M/M_e = 10$, then $\delta L/L = 0.32$ (a 32% fluctuation in tube length), and if $M/M_e = 100$, then $\delta L/L = 0.1$ (a 10% fluctuation). Thus, tube leakage effect is large unless $M/M_e > 100$.

Exact analysis of tube leakage is extremely complicated. Doi[22] and Noolandi and Bernard[27] proposed approximate analyses. Doi[22] obtained

$$\eta_0 = 9.6\eta_0(M_c)(M/M_c)^3(1 - 1.04(M_c/M)^{0.5})^3 \quad (32)$$

This is the Doi equation, which reasonably agrees with the $n = 3.4$ empirical relation in the range $20 < M/M_c < 100$. However, it greatly underestimates the η_0 for $M/M_c < 20$, as can be seen in Figure 12. At very high molecular weights, eq 32 gives $n = 3$ and reduces to eq 29 as it should.

Alternatively, we propose that the tube leakage can be accounted for by

$$\tau_d^{(F)} = \tau_d^{(NF)} \exp\{\beta(1 - (M_c/M)^{0.5})\} \quad (33)$$

where $\tau_d^{(F)}$ is the tube disengagement time with fluctuation considered, $\tau_d^{(NF)}$ is that without considering fluctuation, and β is a numerical constant to be determined later. This relation is suggested by

$$\tau_d^{(F)} \simeq (\bar{L} - \delta L)^2\xi_R/(\pi^2 kT) \quad (34)$$

where ξ_R is the friction coefficient of a Rouse chain, with the assumption that the effect of tube leakage diminishes exponentially. We thus obtain

$$\eta_0 = \eta_0(M_c)(M/M_c)^3 \exp\{2.26(1 - (M_c/M))^{0.5}\} \quad (35)$$

where $\beta = 2.26$ is obtained by requiring that eq 35 reduce to eq 29 at $M \to \infty$.

Equations 29, 32, and 35 are plotted together and compared with experimental data for FEPs and polystyrenes in Figure 12. All three equations converge at very high molecular weights. However, in the conventional molecular weight range, eq 29 overestimates the η_0 and eq 32 underestimates it, while eq 35 correctly predicts the η_0 over the entire molecular weight range.

The reduced plot (Figure 12) is a universal master curve, since $\eta_0/\eta_0(M_c)$ vs. M/M_c is independent of temperature and chemical composition. We choose to examine the relationship with polystyrenes in addition to the present FEPs, since polystyrenes are perhaps the most widely and accurately studied. Several workers have accurately measured the η_0 on the same narrow-distribution polystyrenes. The data were extensively reviewed and compared before.[26] Four sets of polystyrene data are chosen to be particularly accurate, i.e., the data of Onogi and co-workers[14] by dynamic rheometry (160 °C), of Akovali[29] by stress relaxation (129 °C), of Tobolsky and co-workers[30] by stress relaxation (100 °C), and of Fox and Flory[31] by shear flow (217 °C). The data of Tobolsky and co-workers[30] are nearly identical with those of Akovali,[29] but the latter extend over wider molecular weight ranges. For legibility, therefore, the data of Tobolsky and co-workers are not shown in Figure 12. As can be seen, eq 35 adequately represents the η_0 over the entire molecular weight range for $M/M_c > 1$ for both the FEPs and polystyrenes.

It is particularly interesting to note that eq 35 predicts a significant curvature near $M/M_c = 1$ and that this curvature is indeed verified by the experimental data. Equation 35 also indicates that $n = 4.1$ at $M = M_c$, which gradually decreases to the asymptotic value of $n = 3$ at $M \to \infty$. In the conventional molecular weight range (M/M_c = 1–100), the η_0 values predicted by eq 35 give $n = 3.5$ when fitted by least squares, in agreement with the empirical results. Figure 13 shows the n values as a function of M/M_c, as predicted by eq 35.

Furthermore, we note that the $\eta_0(M_c)$ predicted by eq 30 is 2.29 P, which is indeed greater than the value of 0.229 P predicted by eq 35 by a factor of about 9.6, as expected.

Conclusion

Linear viscoelastic properties in the terminal and plateau zones for four tetrafluoroethylene–hexafluoropropylene copolymers (FEPs) in the amorphous melts are measured by dynamic rheometry. The storage modulus master curves are deconvoluted to obtain the molecular weight distributions, which are analyzed to show that the free radical polymerization of these fluoro polymers proceeds essentially by binary coupling of chain ends with a skew toward high molecular weights.

The steady-state compliance is determined from the relaxation time spectrum in the terminal zone. Doi–Edwards theory adequately predicts the values for monodisperse polymers but overestimates the polydispersity effect. On the other hand, the Mills equation adequately predicts the polydispersity effect. Combination of the Doi–Edwards equation for monodisperse polymer and the

Mills equation for polydispersity gives eq 26, which adequately predicts the steady-state compliance for polydisperse polymers.

The present FEPs have very high molecular weights (M_w/M_c = 29–77) and are indeed found to verify the η_0 vs. M^3 relation predicted by the reptation theory. At lower molecular weights (M_w/M_c = 1–50), however, the empirical η_0 vs. $M_w^{3.4}$ relation holds. This is explained by the fluctuation of tube contour length (tube leakage). Consideration of the tube leakage effect in the reptation theory gives a relation that correctly predicts the molecular weight dependence of zero-shear viscosity over the entire molecular weight range ($M/M_c > 1$). That is, in the relation $\eta_0 = \eta_0(M_c)(M/M_c)^n$, n = 4.1 at $M = M_c$ and asymptotically decreases to n = 3 at $M \rightarrow \infty$.

Acknowledgment. The author thanks Dr. Howard W. Starkweather, Jr., for helpful discussions during the course of this work.

Registry No. Tetrafluoroethylene, 116-14-3; hexafluoropropylene, 116-15-4; (tetrafluoroethylene)·(hexafluoropropylene) (copolymer), 25067-11-2.

References and Notes

(1) Wu, S. *Polym. Eng. Sci.* **1985**, *25*, 122.
(2) Wu, S. In "Advances in Rheology, Volume 3. Polymers"; Mena, B., Garcia-Rejon, A., Rangel-Nafaile, C., Eds.; Universidad Nacional Autonoma de Mexico: Mexico, 1984; pp 359–366. Proceedings of IX International Congress of Rheology, Acapulco, Mexico, Oct. 1984.
(3) Doi, M.; Edwards, S. F. *J. Chem. Soc., Faraday Trans. 2* **1978**, *74*, 1789, 1802, 1818; **1979**, *75*, 38.
(4) Rouse, P. E., Jr. *J. Chem. Phys.* **1953**, *21*, 1272.
(5) McCrum, N. G.; Read, B. E.; Williams, G. "Anelastic and Dielectric Effects in Polymeric Solids"; Wiley: New York, 1967; pp 460–461.
(6) Ajroldi, G.; Garbuglio, C.; Ragazzini, M. *J. Appl. Polym. Sci.* **1970**, *14*, 79.
(7) Case, L. C. *Polym. Lett.* **1963**, *1*, 345; *J. Appl. Polym. Sci.* **1960**, *3*, 254.
(8) Tobolsky, A. V.; Katz, D.; Takahashi, M. *J. Polym. Sci., Part A* **1963**, *1*, 483.
(9) Nishioka, A.; Watanabe, M. *J. Polym. Sci.* **1957**, *24*, 298.
(10) Wu, S. "Polymer Interface and Adhesion"; Marcel Dekker: New York, 1982; pp 377–379.
(11) Nielsen, L. E. "Polymer Rheology"; Marcel Dekker: New York, 1977; pp 31–36.
(12) Ferry, J. D. "Viscoelastic Properties of Polymers", 3rd ed.; Wiley: New York, 1980.
(13) Graessley, W. W. *Adv. Polym. Sci.* **1974**, *16*, 1.
(14) Onogi, S.; Masuda, T.; Kitagawa, K. *Macromolecules* **1970**, *3*, 109.
(15) Masuda, T.; Kitagawa, K.; Onogi, S. *Polym. J. (Tokyo)* **1970**, *1*, 418.
(16) Raju, V. R.; Menezes, E. V.; Marin, G.; Graessley, W. W.; Fetters, L. J. *Macromolecules* **1981**, *14*, 1668.
(17) Elias, H.-G. "Macromolecules. I. Structure and Properties"; Plenum Press: New York, 1977; pp 287 ff.
(18) Graessley, W. W. *J. Polym. Sci., Polym. Phys. Ed.* **1980**, *18*, 27.
(19) Mills, N. J. *Eur. Polym. J.* **1969**, *5*, 675.
(20) Zosel, A. *Rheol. Acta* **1971**, *10*, 215.
(21) Berry, G. C.; Fox, T. G. *Adv. Polym. Sci.* **1968**, *5*, 261.
(22) Doi, M. *J. Polym. Sci., Polym. Phys. Ed.* **1983**, *21*, 667.
(23) Bernard, D. A.; Noolandi, J. *Macromolecules* **1982**, *15*, 1553.
(24) Friedman, E. M.; Porter, R. S. *Trans. Soc. Rheol.* **1975**, *19*, 493.
(25) Prest, W. M.; Porter, R. S. *Polym. J. (Tokyo)* **1973**, *4*, 154.
(26) Casale, A.; Porter, R. S.; Johnson, J. F. *J. Macromol. Sci., Rev. Macromol. Chem.* **1971**, *C5*, 387.
(27) Noolandi, J.; Bernard, D. A. *Can. J. Phys.* **1983**, *61*, 1035.
(28) Graessley, W. W. *Adv. Polym. Sci.* **1982**, *47*, 67.
(29) Akovali, G. *J. Polym. Sci., Part A-2* **1967**, *5*, 875.
(30) Tobolsky, A. V.; Aklonis, J. J.; Akovali, G. *J. Chem. Phys.* **1965**, *42*, 723.
(31) Fox, T. G.; Flory, P. J. *J. Polym. Sci.* **1954**, *14*, 315; *J. Phys. Chem.* **1951**, *55*, 221.

New Model of the Origin of the Stereospecificity in the Synthesis of Syndiotactic Polypropylene

Paolo Corradini, Gaetano Guerra,* and Rachele Pucciariello

Dipartimento di Chimica, Università di Napoli, 80134 Napoli, Italy.
Received January 22, 1985

ABSTRACT: A new model is suggested for the origin of the syndiospecificity in the Ziegler–Natta polymerization of propene by homogeneous catalytic systems. Nonbonded energy calculations for possible diastereoisomeric situations at the proposed catalytic site are reported. In our model, the configuration of the last added monomeric unit influences directly the chirality (Λ or Δ) of an octahedral catalytic intermediate; such chirality, in turn, determines the configuration of the entering monomeric unit.

Introduction

The problem of the origin of syndiotactic stereoregulation in the polymerization of propene in the presence of homogeneous catalytic systems (e.g., VCl_4–AlR_2Cl or –$AlRCl_2$, where R = alkyl group) has been relatively little investigated up to now.

It has been established that the syndiotactic polymerization of propene is not completely regiospecific and that it must be formally considered as a binary copolymerization of head-to-tail and tail-to-head propene units;[1,2] moreover, the only syndiospecific step would be the insertion of the monomer into a metal–secondary carbon bond, with formation of a new secondary metal–carbon bond.[1-3]

All the proposed models for syndiotactic propagation suppose that the active center is a metal–carbon bond and that the monomer first coordinates to the metal atom; moreover, all of them attribute the stereospecificity to steric factors. However, different driving forces for the syndiospecificity have been proposed.

According to the model of Arlman and Cossee,[4] there are two adjacent accessible positions at the catalytic site, one for the growing chain and one for the incoming monomer. The two positions favor the coordination of the propene monomer with opposite prochiral faces; if the growing polymer chain alternates between the two positions at each insertion step, syndiotactic propagation is ensured. An analogous model has been proposed for the ring-opening polymerization of norbornene derivatives by $ReCl_5$, where the propagation species is a metallocarbene complex.[5]

Most of the authors[3,6,7] favored instead the hypothesis that the syndiotacticity is due to steric repulsions between the methyl group of the complexed propene and the last

0024-9297/85/2218-2030$01.50/0